Nuclear Inst. and Methods in Physics Research, A 996 (2021) 165132

Contents lists available at ScienceDirect

Nuclear Inst. and Methods in Physics Research, A

journal homepage: www.elsevier.com/locate/nima

Diffracted transition radiation as a new diagnostic tool for relativistic electron beam emittance

Yu.A. Goponov [a], R.A. Shatokhin [a], K. Sumitani [b], Y. Takabayashi [c], I.E. Vnukov [a,*]

[a] Belgorod National Research University, 85 Pobedy str., 308015 Belgorod, Russia
[b] Japan Synchrotron Radiation Research Institute (JASRI), 1-1-1 Kouto, Sayo-cho, Sayo-gun, Hyogo 679-5198, Japan
[c] SAGA Light Source, 8-7 Yayoigaoka, Tosu, Saga 841-0005, Japan

ARTICLE INFO

Keywords:
Beam diagnostics
Beam size
Crystal
Parametric X-ray radiation
Diffracted transition radiation

ABSTRACT

The possibility of determining the emittance of a beam of relativistic electrons by measuring two-dimensional angular distributions of diffracted transition radiation of relativistic electrons for two distances between the crystal where the radiation is generated and the coordinate detector is considered. It is shown that the technique enables the determination of the transverse dimensions and, in the case of a mismatch between the symmetry planes of the beam and the horizontal and vertical planes, their rotation angle. A technique is proposed for determining the beam divergence by comparing the measured angular distribution of the diffracted transition radiation with a model. The sought values of the divergence are determined from the results of "fitting", where the fitted function is the distribution for a larger distance, and the fitting function is the convolution of a model angular distribution with a two-dimensional Gaussian distribution describing the diverging electron beam. The conditions and boundaries of its practical implementation for measuring the emittance of the beam of planned electron–positron colliders at the intermediate stage of acceleration are analyzed.

1. Introduction

To date, many destructive [1] and non-destructive [2,3] methods have been developed to determine the transverse sizes of an electron (positron) beam from linear accelerators by employing visible light from fluorescent screens and optical transition radiation (OTR) or optical diffraction radiation (ODR) from metal foils set in the accelerator. However, optical radiation does not ensure measurement of extremely small beam sizes for electron–positron linear colliders such as the International Linear Collider (ILC) [4] and the Compact Linear Collider (CLIC) [5] because OTR and ODR become coherent under these conditions [6]. Wire scanners [7,8] are not capable of working with beams of such small sizes, either.

The so-called Shintake monitor [9] is considered to be the most promising beam size measurement method for linear colliders. However, it cannot be used in a collider regime where there are two simultaneous particle beams or for intermediate diagnostics and control of the beams inside the accelerator during the acceleration process.

A possible solution to this problem is to determine the size of the beam $\sigma_{x,y}$ on the basis of its divergence $\theta_{x,y}$ and the normalized emittance $\gamma\epsilon_{x,y}$, calculated or measured in the early stages of acceleration [10]. Here, $\epsilon_{x,y} = \sigma_{x,y}\theta_{x,y}$, and γ is the Lorentz factor. The abovementioned coherent effects in the optical radiation requires the use of radiation with a shorter wavelength to determine the beam divergence, in particular, diffracted transition radiation (DTR) [10] or diffracted diffraction radiation (DDR) [11] in the X-ray frequency range, generated when relativistic electrons pass through or near fine perfect crystals [10] or X-ray mirrors [11]. To date, many beam diagnostic methods to measure beam sizes and divergences have been proposed using X-rays such as PXR [12,13] and DTR [14–17].

PXR can be considered as coherent scattering of the field of a fast charged particle by the electron shells of the periodically located atoms of a crystal [18]. It is quasi-monochromatic, has a relatively narrow angular distribution with a characteristic emission angle $\Theta_{ph} = \sqrt{\gamma^{-2} + \omega_p^2/\omega^2}$ [19], where ω and ω_p are the energies of the photon and plasmon of the medium, respectively, and are emitted at an angle $\Theta_D = 2\Theta_B$ with respect to the direction of particle motion, where Θ_B is the angle between the direction of the electrons and the diffraction plane.

Recently, we proposed a technique for determining the transverse dimensions of an electron beam by measuring the PXR angular distributions for two different distances between the crystal and the coordinate detector [20]. In [21], the simulation of determining the beam dimensions by the [20] method was carried out. It was shown that the error associated with using this method to estimate the beam dimensions did

* Corresponding author.
E-mail address: vnukov@bsu.edu.ru (I.E. Vnukov).

https://doi.org/10.1016/j.nima.2021.165132
Received 29 October 2020; Received in revised form 3 February 2021; Accepted 7 February 2021
Available online 10 February 2021
0168-9002/

not exceed 5%–7%, and the minimum measured dimensions $\sigma_{x,y}$ were determined by the conditions $\sigma_{x,y} > \delta$ and $\sigma_{x,y}/R_2 > 0.1\Theta_{ch}$, where δ is the pixel size of the coordinate detector, R_2 is the shorter distance between the crystal and the detector, and Θ_{ch} is the characteristic radiation angle. The minimum measured transverse dimensions are limited by the distance between the detector and the electron beam and cannot be less than 50–100 μm [21].

The PXR intensity reaches saturation for electron energies of the order of 1 GeV and below, depending on the energy of the emitted radiation, and the characteristic angle of photons emission is typically significantly greater than γ^{-1}, therefore its use to determine the electron beam divergence $\theta_e \sim \gamma^{-1}$ and below is impractical.

In the same direction as the PXR, diffracted transition radiation is emitted, which can be represented as the reflection of transition radiation (TR) occurring on the front face of the crystal [22]. At electron energies above 5 GeV, the angular density of the DTR with a characteristic emission angle $\Theta_{ch} \sim \gamma^{-1}$ [18] is much higher than the angular density of PXR [14–16] whose contribution to these electron energies can be neglected. Therefore, the minimum transverse dimensions that can be measured using the method in [20] sharply decrease and are limited mainly by the dimensions of the coordinate detector element, that is, the minimum measurable value $\sigma_{x,y} \sim \delta \approx$ 10–15 μm [21].

If it were possible, from the measurement results of angular distributions of DTR, to estimate not only the transverse dimensions of the beam by the technique in [20], but also its divergence and the angle of rotation of the beam symmetry plane relative to the horizontal plane, then this would significantly expand its capabilities and ease of use. Based on the foregoing, an investigation into expanding the possibilities of the technique in [20] to determine the emittance of electron beams with energies of the order of 10 GeV and into the limits of this technique's applicability seems important and urgent.

2. Theoretical consideration

A schematic representation of the process of formation, distribution and registration of the DTR is shown in Fig. 1. The electron beam falls on the crystal and generates transition radiation as it enters it. Photons of transition radiation with energy ω and direction of propagation $\vec{n}$, satisfying Bragg's law, are reflected on crystal planes rotated through the Bragg angle Θ_B relative to the direction of incidence of the electron beam, move in the direction of Bragg scattering $\vec{n}'$ and are recorded by a detector located at an angle $\Theta_D = 2\Theta_B$ relative to the direction of the electron beam. Hereinafter, it is assumed that the spatial distribution of particles relative to the center of the beam and its angular distribution are described by two-dimensional Gaussian distributions with characteristic sizes σ_x, σ_y and divergence angles θ_x, θ_y (1σ).

The resulting distribution of radiation, recorded by a coordinate detector located at a distance R from the crystal depends on the angular distribution of the transition radiation, the angular distribution of the electron beam generating this radiation, the spatial distribution of the points of electron hitting the crystal and the distance between the crystal and the detector. In particular, with a decrease in the distance between the crystal and the detector, the influence of the contribution of the beam transverse dimensions on the recorded distribution of the points of impact of photons on the detector increases sharply, which is the basis of the method for determining the transverse dimensions of the electron beam from the results of measuring the angular distributions for two distances between the crystal and the detector [20].

Let us analyze successively the influence of these factors on the recorded radiation distribution. In accordance with [15,23,24], the spectral–angular distribution of the DTR from a monodirectional electron beam incident on the crystal at an angle Θ_B relative to the reflecting planes, can be written as:

$$\frac{d^2 I_{DTR}}{d\omega d\Omega'} = \int d\omega \int \frac{d^2 I_{TR}}{d\omega d\Omega} R(\vec{n} \to \vec{n}', \omega, \vec{g}) d\Omega, \quad (1)$$

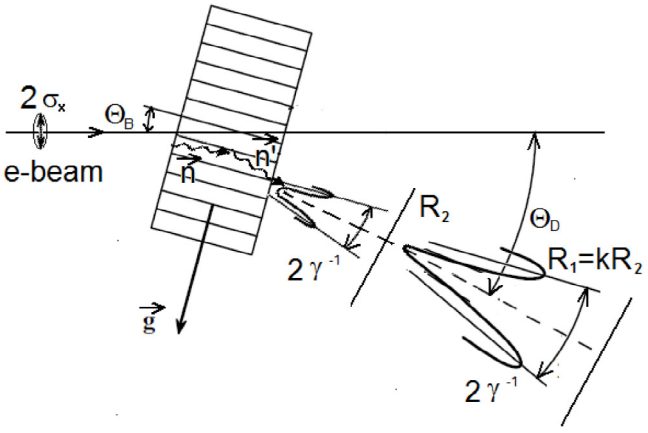

Fig. 1. A schematic representation of the process of formation, distribution and registration of the DTR.

where $d^2 I_{TR}/d\omega d\Omega$ is the transition radiation spectral–angular distribution, $R(\vec{n} \to \vec{n}', \omega, \vec{g})$ is the reflecting ability of the crystal. Here $\vec{n}$ and $\vec{n}'$ are unit vectors in the direction of motion of the primary and reflected photons, determined in coordinate systems related to the directions of the electron beam and Bragg scattering (see [20] for details). $\vec{g}$ is the reciprocal lattice vector of the plane on which the reflection occurs. Its direction is determined by the angle of rotation of the plane relative to the direction of the electron beam.

The energy of the reflected photon is related to the angle between the vectors $\vec{n}$ and $\vec{g}$ via $\omega = \frac{|\vec{g}|^2}{2\sqrt{\varepsilon_0}|\vec{n}\vec{g}|}$, where $\varepsilon_0 = 1 - \omega^2/\omega_p^2$ is the dielectric constant of the crystal substance. Integration is performed over all angles and energies of photons that satisfy the Bragg condition. To simplify the problem, we will assume that the reflecting plane is oriented vertically, that is, the vector $\vec{g}$ lies in the horizontal plane.

The width of the reflected radiation spectrum (see, for example, [15, 24]) can be written as $\Delta\omega = \omega \cos\Theta / \sin\Theta \Delta\theta$, where $\Delta\theta$ is the width of the so-called Darwin table, and Θ is the angle between the direction of motion of the photons and the crystal plane. For $\omega \sim 10$ keV and above, $\Delta\theta \sim \frac{(\omega_p/\omega)^2}{\sin 2\Theta_B} \approx 10^{-4} - 10^{-5}$.

Taking into account the angular distribution of the transition radiation and the divergence of the electron beam, the energy of reflected photons can be written as $\omega = \omega_B(1 + (\vartheta_\gamma^{\parallel} + \Theta_e^{\parallel})\cos\Theta_B / \sin\Theta_B)^{-1}$, where $\omega_B = \frac{|\vec{g}|}{2\sin\Theta_B}$, and $\vartheta_\gamma^{\parallel}$ and $\Theta_e^{\parallel}$ are the projections of, respectively, the vectors $\vec{n}$ and the unit vector along the direction of motion of the electrons incident on the crystal $\vec{n}_e$ in the direction of the vector $\vec{g}$ [22]. As a result of these factors, the width of the diffracted radiation spectrum increases to $\Delta\omega \approx \omega_B(\vartheta_\gamma^{\parallel} + \Theta_e^{\parallel})\cos\Theta_B / \sin\Theta_B$. Assuming that the divergence of the electron beam is of the order of γ^{-1} and considering that for angles of photons emission greater than 2–3 γ^{-1} the intensity of TR drops sharply, we can assume that for an electron energy of the order 10 GeV and observation angles $\Theta_D \approx 2\Theta_B > 20°$ monochromaticity of the reflected radiation spectrum emitted in a full cone $\Delta\omega/\omega \le 5\cos\Theta_B / \sin\Theta_B \gamma^{-1} \sim 10^{-3}$.

Consequently, the diffracted transition radiation can be considered to be monochromatic, and instead of the spectral–angular distribution $\frac{d^2 I_{DTR}}{d\omega d\Omega'}$, we will focus on the angular distribution DTR $J(\omega_B, \vartheta'_x, \vartheta'_y)$, where ϑ'_x and ϑ'_y are the angles of photon emission in, respectively, the horizontal and vertical directions, measured relative to the center of the reflex located at an angle $\Theta_D = 2\Theta_B$ relative to the direction of the electron beam.

It is known (see, for example, [15,16,25]) that when a crystal thickness T is more than several lengths of primary extinction $l_{ext} \sim$ 10 μm and the condition $\Delta\theta \ll \gamma^{-1}$ is satisfied, the angular distribution

of the DTR can be represented as:

$$J_{\mathrm{DTR}}(\omega_{\mathrm{B}}, \vartheta'_x, \vartheta'_y) = N_{\mathrm{DTR}}(\omega_{\mathrm{B}}) \frac{C_{\mathrm{pol}} \vartheta'^2_x + \vartheta'^2_y}{\left((\vartheta'^2 + \Theta^2_{\mathrm{ph}})(\vartheta'^2 + \gamma^{-2})\right)^2}, \tag{2}$$

where $\vartheta'^2 = \vartheta'^2_x + \vartheta'^2_y$, $N_{\mathrm{DTR}}(\omega_{\mathrm{B}})$ is a factor that characterizes the output of the DTR and that depends on the crystal used, the observation angle, and the order of reflection. C_{pol} is a polarization factor equal to $\cos^2 2\Theta_{\mathrm{B}}$ and $\cos 2\Theta_{\mathrm{B}}$ in the framework of the kinematic [25] and dynamic [15,16] theories of X-ray diffraction in crystals, respectively. The presence of this factor is due to the dependence of the reflectivity of the crystal on the radiation polarization associated with the azimuthal angle of emission of the transition radiation photons φ measured from the plane containing the vectors $\vec{n}_e$ and $\vec{N}$, where $\vec{N}$ is normal to the crystal surface [26]. In our case, this is a horizontal plane.

The angular distribution of DTR for a point-like diverging electron beam $J_{\mathrm{DTR}}(\omega_{\mathrm{B}}, \vartheta_y, \vartheta_x)$ (see, for example, [10,15]) can be written as follows:

$$J_{\mathrm{DTR}}(\omega_{\mathrm{B}}, \vartheta_y, \vartheta_x) = \iint J_{\mathrm{DTR}}(\omega_{\mathrm{B}}, \vartheta'_y, \vartheta'_x)$$

$$G_e(\vartheta'_y \to \vartheta_y, \vartheta'_x \to \vartheta_x) d\vartheta'_y d\vartheta'_x, \tag{3}$$

where $J_{\mathrm{DTR}}(\omega_{\mathrm{B}}, \vartheta'_y, \vartheta'_x)$ is the angular distribution of the diffracted transition radiation (expression (2)), and $G_e(\vartheta'_y \to \vartheta_y, \vartheta'_x \to \vartheta_x)$ is a two-dimensional Gaussian distribution describing a diverging electron beam:

$$G_e(\vartheta'_y \to \vartheta_y, \vartheta'_x \to \vartheta_x) = \frac{1}{2\pi\theta_y\theta_x}$$

$$\exp\left(\frac{-(\vartheta_y - \vartheta'_y)^2}{2\theta^2_y}\right) \exp\left(\frac{-(\vartheta_x - \vartheta'_x)^2}{2\theta^2_x}\right), \tag{4}$$

where θ_x and θ_y are characteristic angles of beam divergence in the horizontal and vertical directions, respectively.

In general, a coordinate detector measures the spatial distribution of the points where particles or quanta hit it. In the case of a radiation source of small dimensions or a large distance between the detector and the source, when its dimensions can be neglected, measurements are typically in terms of the angular distribution of radiation. Since the transverse dimensions of the electron beam of interest do not exceed several tens of microns, and the minimum possible distance between the crystal and the detector is more than several tens of centimeters (see, for example, [21]), we do not differentiate between the spatial and angular distributions and discuss the angular distribution of radiation for both point-like and extended electron beams.

The influence of the beam size and the distance between the crystal and the detector R on the measured two-dimensional angular distribution of radiation (see, for example, [13]) can be expressed as follows:

$$J_R(\omega_{\mathrm{B}}, \vartheta'_y, \vartheta'_x) = \iint J(\omega_{\mathrm{B}}, \vartheta_y, \vartheta_x)$$

$$G(\vartheta_y \to \vartheta'_y, \vartheta_x \to \vartheta'_x) d\vartheta_y d\vartheta_x, \tag{5}$$

where $J(\omega_{\mathrm{B}}, \vartheta_y, \vartheta_x)$ and $J_R(\omega_{\mathrm{B}}, \vartheta'_y, \vartheta'_x)$ are the angular distributions of radiation for a point-like and extended beam of particles on the target, respectively, and the integration is carried out within the full solid angle. The function $G(\vartheta_y \to \vartheta'_y, \vartheta_x \to \vartheta'_x)$ describes the relationship between the variables of each of these distributions and, for a two-dimensional Gaussian distribution of the points of electrons hitting the crystal, can be written as:

$$G(\vartheta_y \to \vartheta'_y, \vartheta_x \to \vartheta'_x) = \frac{1}{2\pi\sigma'_y\sigma'_x}$$

$$\exp\left(\frac{-(\vartheta_y - \vartheta'_y)^2}{2(\sigma'_y)^2}\right) \exp\left(\frac{-(\vartheta_x - \vartheta'_x)^2}{2(\sigma'_x)^2}\right), \tag{6}$$

where $\sigma'_x = \sigma_x/R$, $\sigma'_y = \sigma_y/R$ are the effective angles of divergence in the horizontal and vertical planes, respectively, and R is the distance between the crystal and the detector. This form for recording the relationship between the angle of photon emission for point-like and extended emission sources is considered reasonable due to the fact that for a fixed angle of the detector and small observation angles (less than 30–40 degrees), the change in the spatial position of the emitting point is practically equivalent to the corresponding change in the angle of photon emission (see [20] for details). Thus, due to the small size of the beam on the crystal and the relatively large distance between the crystal and the detector, the change in the solid angle covered by the detector element can be neglected.

As can be seen from expressions (5) and (6), a change in the distance between the crystal and the detector leads to a change in the recorded angular distribution of the radiation yield, which forms the basis of the method for determining the beam size from the angular distributions of radiation for two distances between the crystal and the coordinate detector [20].

3. Description of method

Here is a brief description of the method for estimating the beam size on a crystal on the basis of [20] and [21]. It is assumed that the angular distributions of DTR are measured by a coordinate detector similar to the X-ray detector [27] used in the experiment in [28]. The device measures integral intensity of the incident radiation and the signal amplitude recorded by each pixel is proportional to the energy left in it by the photons of the recorded radiation. This makes it possible to measure the beam parameters rapidly. The photon energy is not recorded, so we will omit ω_{B} and discuss only the angular distribution of radiation.

Below we will consider the determination of the beam parameters for the reflecting plane (011) of a silicon crystal and the observation angle $\theta_{\mathrm{D}} = 32.2°$. When the condition $\omega \ll \gamma\omega_{\mathrm{p}}$ is satisfied, the angular distribution of the intensity of the transition radiation, and hence the DTR, does not depend on the photon energy; therefore, all of the following statements apply to other crystals, observation angles, and reflecting planes. Choosing a different crystal or observation angle will only change the photon energy and reflected radiation yield [29]. The presence of the polarization factor C_{pol} in expression (2) leads to a change in the ratio of the intensities of the vertical and horizontal distributions with a change in the observation angle. Transition radiation does not depend on the sign of the particle charge [18,26], therefore, the technique works for both electron and positron beams.

For a coordinate detector located at a distance R, the measured two-dimensional angular distribution of the radiation intensity $Y_R(\theta_{y_i}, \theta_{x_j})$ can be written in the following form:

$$Y_R(\theta_{y_i}, \theta_{x_j}) = \iint_{\Delta\Omega(y_i, x_j)} J_R(\vartheta'_y, \vartheta'_x) d\vartheta'_y d\vartheta'_x, \tag{7}$$

where $J_R(\vartheta'_y, \vartheta'_x)$ is defined in expressions (5) and (6). $\Delta\Omega(y_i, x_j)$ is the solid angle covered by the coordinate detector element located at the angles θ_{y_i} and θ_{x_j} at the point y_i, x_j, over which the integration is performed.

It is clear that the difference between the distributions $Y_{R_1}(\theta_{y_i}, \theta_{x_j})$ and $Y_{R_2}(\theta_{y_i}, \theta_{x_j})$, measured for the distances R_1 and R_2 and normalized to the same number of particles passing through the crystal is due only to the characteristic dimensions of the beam and the distances between the crystal and the detector. These distributions themselves are the results of convolutions of the angular distribution for a point-like beam of particles $J(\vartheta_y, \vartheta_x)$ and two two-dimensional Gaussian distributions with standard deviations $\sigma'_{x_1,y_1} = \sigma_{x,y}/R_1$ and $\sigma'_{x_2,y_2} = \sigma_{x,y}/R_2$. As a

first approximation, we can assume that $Y_{R_2}(\theta_{y_i}, \theta_{x_j})$ is the convolution of the distribution $Y_{R_1}(\theta_{y_i}, \theta_{x_j})$ with a Gaussian distribution with a variance that depends on the unknown size of the beam on the target and the quantities R_1 and R_2,

We assume that $R_1 = k \cdot R_2$, where k is an integer coefficient not equal to one, and the solid angles covered by the detectors are the same in each measurement. In other words, the value of $Y_{R_1}(\theta_{y_i}, \theta_{x_j})$ at each distribution point is equal to the radiation intensity recorded by a matrix of $k \times k$ elements covering the same solid angle as the detector's element installed at a distance of R_2.

To determine the required beam size on the target, we use the least squares method, minimizing the quadratic form:

$$\sum_{i=1}^{n}\sum_{j=1}^{m}\left(Y_{R_2}(\theta_{y_i}, \theta_{x_j}) - \frac{1}{2\pi\widetilde{\sigma}'_x\widetilde{\sigma}'_y}\sum_{i'=1}^{n}\sum_{j'=1}^{m} Y_{R_1}(\theta_{y_{i'}}, \theta_{x_{j'}})\right)$$

$$\exp\left(\left(-\frac{(\theta_{y_i} - \theta_{y_{i'}})^2}{2(\widetilde{\sigma}'_y)^2}\right)\exp\left(-\frac{(\theta_{x_j} - \theta_{x_{j'}})^2}{2(\widetilde{\sigma}'_x)^2}\right)\right)^2 = \text{Min}, \tag{8}$$

where m and n are the numbers of points in the measured distributions in the horizontal and vertical directions, respectively. $\widetilde{\sigma}'_x$ and $\widetilde{\sigma}'_y$, which are adjustable parameters that minimize this form, are related to the beam size on the target $\widetilde{\sigma}_x$, $\widetilde{\sigma}_y$ via [20,21]

$$\widetilde{\sigma}_{y,x} \approx \frac{k \cdot R_2}{\sqrt{k^2 - 1}}\widetilde{\sigma}'_{y,x}. \tag{9}$$

4. Determination of electron beam parameters

In order to test the capabilities of the technique and determine the boundaries of its applicability, we simulated the determination of the parameters of an electron beam with an energy of 10 GeV from two-dimensional distributions of diffracted transition radiation measured for two distances between the crystal and the coordinate detector, using the variation of convolution parameters. The simulation was carried out using the following conditions: the (022) reflection of a silicon crystal, a viewing angle of 32.2°, and ω_B = 11.6 keV. The size of the detector element was 10 × 10 μm^2.

As an example, Fig. 2 shows the vertical and horizontal sections of the two-dimensional angular distribution passing through the center of the reflected radiation beam for the following conditions. The dimensions of the electron beam on the crystal are σ_x = 40 μm and σ_y = 20 μm. The divergence of an azimuthally symmetric electron beam θ_e = 15 μrad. The distances between the crystal and the coordinate detector are 2 and 4 m.

To obtain the angular distribution of radiation from a point-like electron beam $J_{DTR}(\vartheta_y, \vartheta_x)$, the angular distribution of DTR $J_{DTR}(\vartheta'_y, \vartheta'_x)$ was convolved with a two-dimensional Gaussian distribution describing an electron beam with a divergence angle θ_e = 15 μrad. The angular distributions of the radiation intensity $J_{R_{1,2}}(\vartheta'_y, \vartheta'_x)$ for an extended beam and the distances between the crystal and the detector R_1 = 4 m and R_2 = 2 m are obtained by convolving $J(\vartheta_y, \vartheta_x)$ with a two-dimensional Gaussian distribution with effective divergences $\sigma'_{x_{1,2}} = \sigma_x/R_{1,2}$ and $\sigma'_{y_{1,2}} = \sigma_y/R_{1,2}$. To get the $Y_{R_1}(\theta_{y_i}, \theta_{x_j})$ and $Y_{R_2}(\theta_{y_i}, \theta_{x_j})$ dependencies $J_{R_{1,2}}(\vartheta'_y, \vartheta'_x)$ were assumed to be "noisy" using a uniform distribution in the range of values ±10% at each point, and the dependence $J_{R_1}(\vartheta'_y, \vartheta'_x)$ was additionally compressed in half for each of the coordinates.

The deviation of the beam size values obtained by fitting from the real values does not exceed 5%–6%. The dependence obtained by fitting (the second term in the quadratic expression in (8)) practically coincides with the dependence for a smaller distance (the first term) and thus is not presented.

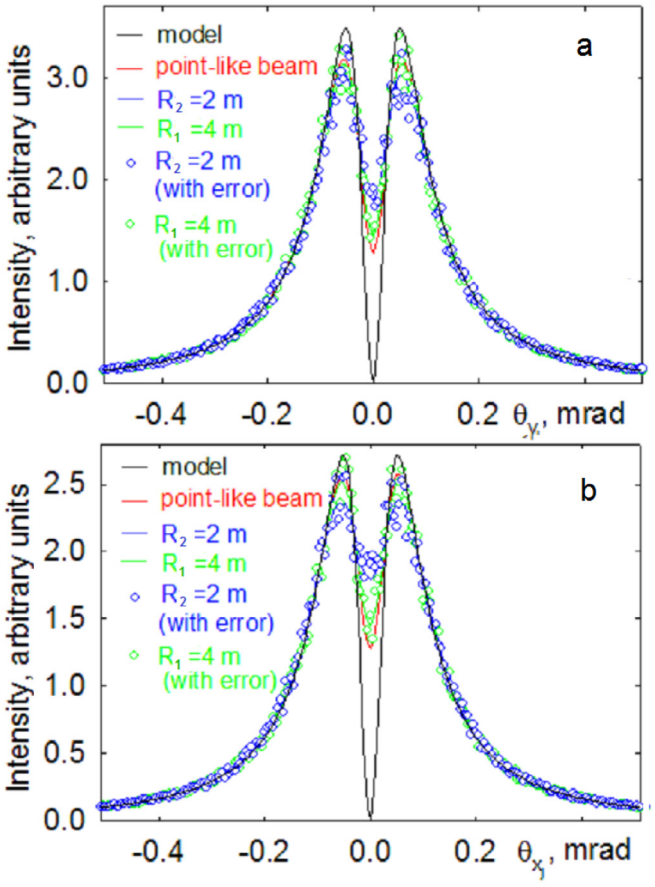

Fig. 2. Angular distribution of radiation in (a) vertical and (b) horizontal directions, showing a model DTR angular distribution, a radiation distribution for a point-like electron beam, and distributions for an extended electron beam with distances R_1 = 4 m and R_2 = 2 m. Electron energy 10 GeV, silicon crystal, (022) reflection order, observation angle Θ_D = 32.2°.

Determination of the beam profile parameters

To determine the sensitivity of the present technique, for the same conditions, we made a cycle of estimates of the beam size obtained using the technique, depending on the distance between the crystal and the detector. During each fitting, the noise implementation was performed anew. The dependence of the beam size estimate $\widetilde{\sigma}_{y,x}$ on the distance, obtained by fitting, is shown in Fig. 3. Here and below, the standard deviation of the values obtained by fitting from the mean is taken as errors. As before, we set $R_1 = 2R_2$.

Fig. 3 shows that for distances R_2 of less than 2 m, the error in determining the vertical size of the beam does not exceed 6%, and the values obtained by fitting coincide with those specified in the simulation. For large distances, the difference between the estimate $\widetilde{\sigma}_y$ and the beam size σ_y = 20 μm increases. At the same time, the fitting error grows. For the horizontal beam size, the deviation is almost half as large, and the increase in fitting error begins for distances of more than 5 m. The arrows indicate the boundaries of the applicability region of the technique for a noise level of 20%. The same behavior was observed for the same electron energy and observation angle in [21] for beam sizes σ_x = 20 and σ_y = 30 μm. In all cases, the differences between the estimate and the true value start to exceed the fitting error under the condition $\sigma'_{x,y} = \sigma_{x,y}/R_2 \le 0.1\gamma^{-1}$.

The reason for this behavior of the fitting results is that the differences between the "noisy" distributions $Y_{R_1}(\theta_x, \theta_y)$ and $Y_{R_2}(\theta_x, \theta_y)$ decrease with increasing distance between the crystal and the coordinate detector [29], so the method loses its sensitivity. It is also found

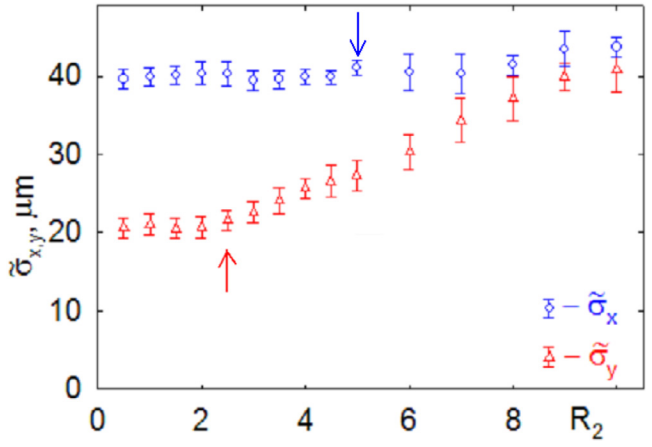

Fig. 3. Dependence of the beam size estimates on the distance between the crystal and the detector. Silicon, electron energy 10 GeV, observation angle $\Theta_D = 32.2°$, $\sigma_x = 40$ μm, $\sigma_y = 20$ μm.

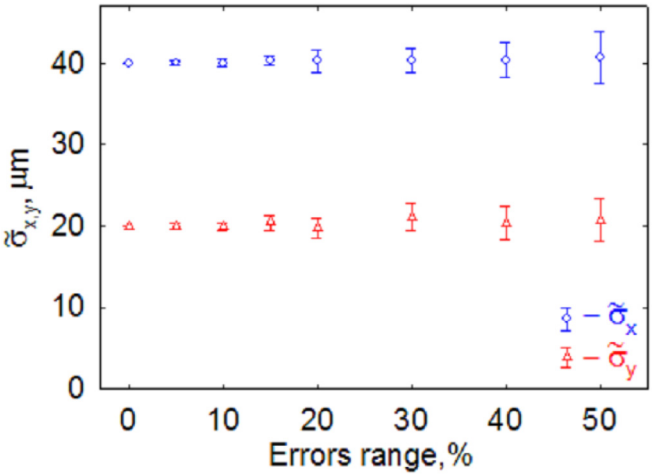

Fig. 4. Dependence of beam size estimates on "noise" level. Silicon, electron energy 10 GeV, observation angle $\Theta_D = 32.2°$, $\sigma_x = 40$ μm, $\sigma_y = 20$ μm.

that with increasing "noise" level, the deviation of $\tilde{\sigma}_{x,y}$ from $\sigma_{x,y}$ begins to manifest itself for smaller distances, and vice versa: with decreasing "noise" level, the fitting error decreases, and the deviation of $\tilde{\sigma}_{x,y}$ from $\sigma_{x,y}$ starts at larger distances. For a horizontal beam size, because of its larger value, an increase in the distance between the crystal and the coordinate detector has a weaker effect on the fitting error and the resulting estimate of the beam size.

To confirm the above, the dependence of $\tilde{\sigma}_{y,x}$ on the noise level obtained by fitting is plotted in Fig. 4 for $\sigma_x = 40$ μm, $\sigma_y = 20$ μm. The distance between the crystal and the detector is 1 and 2 m.

Fig. 4 shows that with an increase in noise level from 10% to 50%, the spread of $\tilde{\sigma}_{x,y}$ values from the true value increased from 2%–3% to 10%–15%. The lower scatter in $\tilde{\sigma}_{x,y}$ in comparison with the noise level is due to the averaging over a large number of points of the analyzed distributions during the fitting process. As a rule, the scatter of experimental data is not less than 10%–15%. Thus, an approximate criterion for the applicability of the method can be the fulfillment of the condition $\sigma'_{x,y} = \sigma_{x,y}/R_2 > 0.1\Theta_{ch}$ as suggested in [20,21]. For the DTR case, $\Theta_{ch} = \gamma^{-1}$.

The electron beam profile (see, for example, [8]) can be rotated around the accelerator axis along the azimuthal angle φ, that is, the semi-major axis of the elliptical beam profile can be rotated relative to the horizontal or vertical planes. In this case, the effective divergences

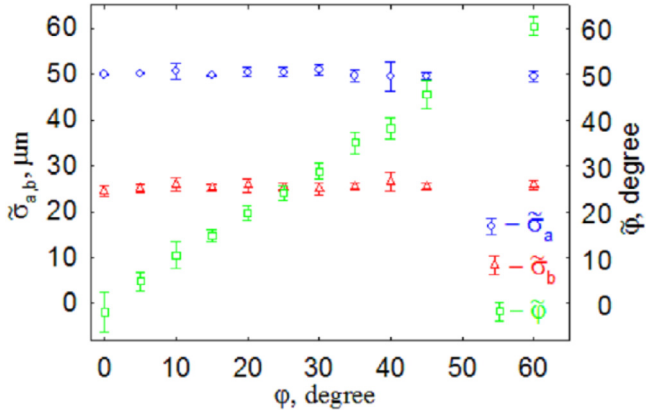

Fig. 5. Dependence of the beam parameter estimates for tilted electron beams on the tilt angle. Silicon, electron energy 10 GeV, observation angle $\Theta_D = 32.2°$, $\sigma_a = 50$ μm, $\sigma_b = 25$ μm.

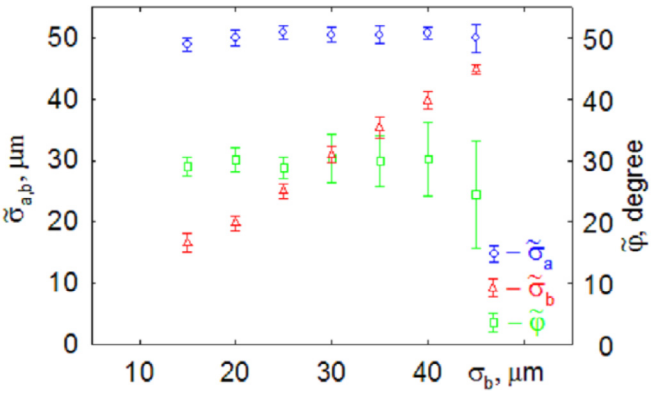

Fig. 6. Dependence of beam parameter estimates for tilted electron beams on σ_b. Silicon, electron energy 10 GeV, observation angle $\Theta_D = 32.2°$, $\sigma_a = 50$ μm, φ=30°.

in Eq. (6) can be rewritten as $\sigma'_x = (\sigma_a \cos\varphi + \sigma_b \sin\varphi)/R$ and $\sigma'_y = (-\sigma_a \sin\varphi + \sigma_b \cos\varphi)/R$, where σ_a and σ_b are, respectively, the major and minor semiaxes of the beam profile, which allows the use of the technique in [20] in this case as well.

Fig. 5 shows the dependence of estimates of the beam size $\tilde{\sigma}_a$, $\tilde{\sigma}_b$ and the tilt angle $\tilde{\varphi}$, obtained through fitting, on the value φ for $\sigma_a = 50$ μm, $\sigma_b = 25$ μm. The calculation is performed for distances $R_1 = 4$ m and $R_2 = 2$ m. All other conditions are the same as those used above.

Fig. 5 shows that estimates of the beam size coincide with the values used in the simulation, and the spread of values does not exceed 3% and 5% for the major and minor semiaxes, respectively. The error in determining the rotation angle does not exceed 2° except at 0°, where it is slightly higher.

To determine the range of applicability of the method for estimating the rotation angle of the symmetry plane of the beam using the proposed technique, Fig. 6 shows the dependence of estimates of beam profile parameters obtained by fitting on σ_b for a rotation angle of 30° and semi-major axis $\sigma_a = 50$ μm.

Fig. 6 shows that the deviation of the values obtained for the transverse dimensions of the beam from the true values does not exceed a few percent. The scatter of the rotation angle values begins to increase starting from $\sigma_b = 30$ μm, which corresponds to a ratio of the beam sizes σ_b/σ_a of 0.6.

It should be recalled that the technique used in [20] is model-independent and, therefore, can be used to determine the profile of an electron beam with the aid of the DTR mechanism or the PXR mechanism. The same approach, that is, estimation of the emitting region size by measuring the angular distributions for two different

distances between the radiation source and the coordinate detector, can be used for any highly directional radiation, including determining the effective transverse dimensions of the emitting region of an X-ray free-electron laser [30].

5. Beam divergence estimate

From the measured angular distribution $Y_{\mathrm{DTR}}(\theta_{y_i}, \theta_{x_j})$, provided one knows the exact form of the angular distribution DTR for a monodirectional electron beam $J_{\mathrm{DTR}}(\vartheta'_y, \vartheta'_x)$, one can estimate the divergence of a point-like electron beam $\theta_{x,y}$ by solving the inverse problem [17]. In practice, this requires the fulfillment of the condition $\sigma'_{x,y} = \sigma_{x,y}/R \ll \theta_{x,y}$, that is, a large distance between the coordinate detector and crystal or small beam sizes. If this condition is not met, then the method in [17] would not be applicable owing to the presence of a systematic error.

To determine the beam divergence, one can use the results of measurements of the angular distributions for two distances to determine the beam sizes $\widetilde{\sigma}_x$, $\widetilde{\sigma}_y$, and then, by taking into account their contribution to the measured angular distribution, estimate the beam divergence $\widetilde{\theta}_x$ and $\widetilde{\theta}_y$.

A comparison of expressions (2)–(6) reveals that the angular distribution of the DTR $Y_R(\theta_{y_i}, \theta_{x_j})$, measured by a detector located at a distance of R, can be represented as two consecutive convolutions of the intrinsic angular distribution of the diffracted transition radiation $J_{\mathrm{DTR}}(\vartheta'_y, \vartheta'_x)$ with the angular distribution of the electron beam $G_e(\vartheta'_y \to \vartheta_y, \vartheta'_x \to \vartheta_x)$ and the effective angular distribution $G(\vartheta_y \to \vartheta'_y, \vartheta_x \to \vartheta'_x)$ caused by the scatter in the locations of electrons hitting the crystal. This allows us to modify the quadratic form (8) and use it to estimate the divergence of an electron beam by the least squares method, where the sought values of the beam divergence $\widetilde{\theta}_x$ and $\widetilde{\theta}_y$ are adjustable parameters that minimize this form.

$$\sum_{i=1}^{n}\sum_{j=1}^{m}\left(Y_R(\theta_{y_i}, \theta_{x_j}) - \frac{\widetilde{C}}{2\pi\sigma''_x\sigma''_y}\sum_{i'=1}^{n}\sum_{j'=1}^{m} J_{\mathrm{DTR}}(\theta_{y_{i'}}, \theta_{x_{j'}})\right)$$

$$\exp\left(\left(-\frac{(\theta_{y_i} - \theta_{y_{i'}})^2}{2(\sigma''_y)^2}\right)\exp\left(-\frac{(\theta_{x_j} - \theta_{x_{j'}})^2}{2(\sigma''_x)^2}\right)\right)^2 = \mathrm{Min}, \qquad (10)$$

where m and n are, as before, the numbers of points of measured distributions in the horizontal and vertical directions, respectively. $J_{\mathrm{DTR}}(\theta_{y_{i'}}, \theta_{x_{j'}})$ is the result of integrating the angular distribution of DTR $J_{\mathrm{DTR}}(\vartheta'_y, \vartheta'_x)$ along the solid angle covered by the detector element located at the point x_i, y_j. $\sigma''_x = \sqrt{(\sigma'_x)^2 + (\widetilde{\theta}_x)^2}$ and $\sigma''_y = \sqrt{(\sigma'_y)^2 + (\widetilde{\theta}_y)^2}$, where $\sigma'_y = \widetilde{\sigma}_y/R$ and $\sigma'_x = \widetilde{\sigma}_x/R$. These are the effective divergences determined through the beam size estimate obtained during the first stage of processing. Here, unlike expression (8), an additional fitting parameter $\widetilde{C}$ appears, because a model dependence is used in the fitting process, rather than an experimental dependence, normalized to the same number of electrons as $Y_R(\theta_{y_i}, \theta_{x_j})$.

As $Y_R(\theta_{y_i}, \theta_{x_j})$, one can take the measurement results for $Y_{R_{1,2}}(\theta_{y_i}, \theta_{x_j})$, used to determine the beam size, or to reduce the error in the obtained values of $\widetilde{\theta}_{x,y}$, carry out an additional measurement. To reduce the influence of the error in determining the transverse dimensions of the beam on the accuracy of the divergence estimate, it is desirable to use the angular distribution measurement results for a larger distance as $Y_R(\theta_{y_i}, \theta_{x_j})$. The same approach can be employed to estimate the beam divergence from the measurement results of the angular distribution of radiation when $\sigma'_{x,y} = \sigma_{x,y}/R \ll \theta_{x,y}$, replacing $\sigma''_{x,y}$ with $\widetilde{\theta}_{x,y}$.

If necessary, during the fitting process, one can take into account the rotation of the beam around the accelerator axis and write $\theta_x = \theta_a \cos\varphi + \theta_b \sin\varphi$ and $\theta_y = -\theta_a \sin\varphi + \theta_b \cos\varphi$, where θ_a and θ_b are the divergences along the symmetry axes of the beam. For small effective divergences ($\sigma_{a,b}/R \ll \theta_{a,b}$), this approach allows determination of the angle of reversal, which is impossible using the methods in [10,17], where only vertical and horizontal distributions of the radiation are analyzed.

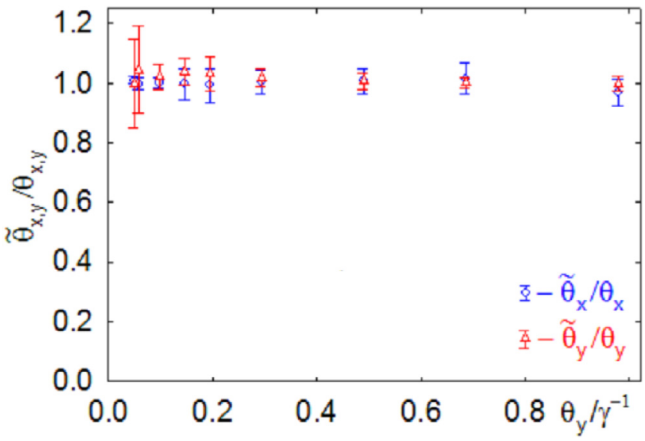

Fig. 7. Dependences of the ratios $\widetilde{\theta}_x/\theta_x$ and $\widetilde{\theta}_y/\theta_y$ on the vertical beam divergence θ_y. Silicon, electron energy 10 GeV, observation angle $\Theta_D = 32.2°$, σ_x=40 μm, σ_y=30 μm. θ_x=15 μrad. R_1=6 m, R_2=3 m.

To simplify quadratic form (10), we combined convolutions according to the divergence and size of the beam on the target. One can perform convolutions (3) and (5) sequentially, and substitute the results in quadratic form (10). The two approaches give roughly the same results. We adopted the approach involving separate computations of convolutions because it appears to be more consistent.

In order to determine the feasibility and limits of applicability of the proposed method for estimating the electron beam divergence, we made a cycle of estimates of the electron beam divergence obtained using this technique and the "noisy" angular distributions for several divergence values. For simplicity, the characteristic beam dimensions on the target σ_x = 40 μm and σ_y = 30 μm are assumed to be known and constant. The beam divergence in the horizontal direction θ_x = 15 μrad. The distances between the crystal and the coordinate detector are 3 m and 6 m. The symmetry planes of the beam coincide with the horizontal and vertical planes. The other conditions are the same as those used above. The dependences of the ratios $\widetilde{\theta}_x/\theta_x$ and $\widetilde{\theta}_y/\theta_y$, obtained by modeling, on the beam divergence in the vertical plane θ_y are plotted in Fig. 7.

Fig. 7 shows that in the investigated range of vertical divergence, the deviation of the divergence estimates obtained by the developed method from the true values does not exceed 4%–5%, with the exception of the range $\theta_y \le 3$ μrad $\sim 0.06\gamma^{-1}$, where the average of the estimates of the vertical divergence $\widetilde{\theta}_y$ is still close to the true value, while the estimation error has grown to ~ 20%.

To reveal why the fitting error increases for small θ_y, Figs. 8(a) and 8(b) show the model vertical angular distributions for θ_y values of 3 and 15 μrad, respectively. All other conditions remain unchanged.

A comparison of Figs. 8(a) and 8(b) reveals that for θ_y = 15 μrad, there is a consistent difference between the model and fitted dependences over the entire range of fitting angles. For θ_y = 3 μrad, a difference is observed only in a narrow range of angles near the center of the reflex, while outside this range, given the "noise" level, there is practically no difference.

Therefore, the increase in error in the estimates of vertical divergence for small θ_y values in Fig. 7 is caused by the scatter in the points of adjusted dependence. This is also evidenced by the fact that as the noise level decreased from ±10% to ±2.5%, the spread in the $\widetilde{\theta}_y$ values obtained for a vertical divergence of 3 μrad dropped from ±14% to ±5%.

This suggests that the proposed method, which enables the estimation of the divergence of an extended electron beam with known transverse dimensions through a comparison of the measured angular distribution of the diffracted transition radiation of relativistic electrons in a thin crystal against a model distribution, can be used if $\theta_{x,y} > 0.1\gamma^{-1}$ for R_1 = 6 m and "noise" level ±10%.

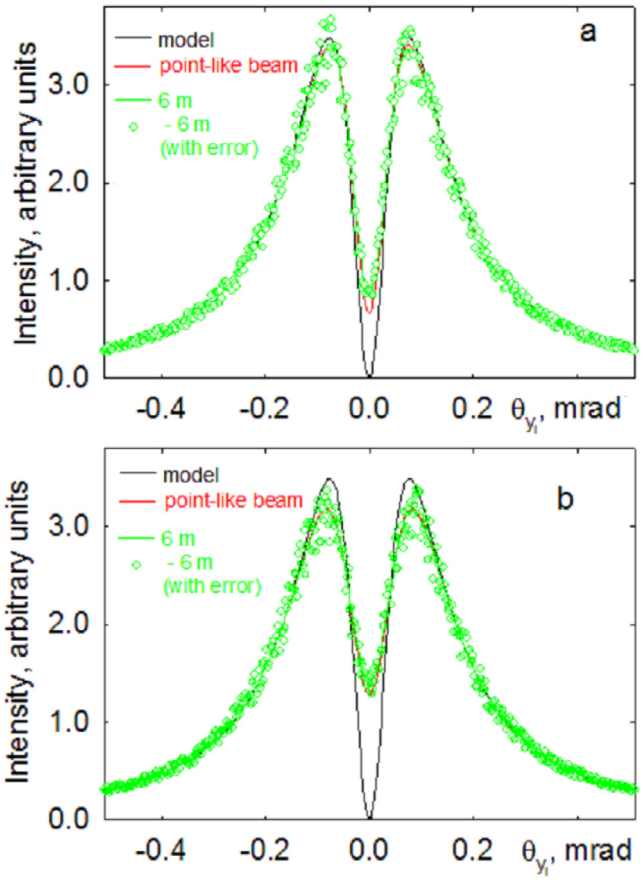

Fig. 8. Angular distributions of radiation in the vertical direction for θ_y=3 μrad (a) and 15 μrad (b), showing a model DTR angular distribution, a radiation distribution for a point-like electron beam, and distributions for the extended electron beam with distance R_1 = 6 m. Electrons energy 10 GeV, silicon crystal, (022) reflection order, observation angle Θ_D = 32.2° σ_x=40 μm, σ_y=30 μm. θ_x=15 μrad.

6. Estimation of beam emittance

The ability to determine the size and divergence of a beam in both directions by measuring the angular distributions of the DTR for two crystal-detector distances raises the possibility of determining the beam emittance from the results of these measurements. In the first stage of processing, the transverse dimensions of the beam $\widetilde{\sigma}_x$ and $\widetilde{\sigma}_y$ are determined from the measurement results, and in the second, according to the results of fitting the model angular distribution to the angular distribution at a greater distance, and taking into account the transverse beam size on the target, the beam's divergence ($\widetilde{\theta}_x$ and $\widetilde{\theta}_y$) and emittance ($\widetilde{\epsilon}_x = \widetilde{\sigma}_x\widetilde{\theta}_x$ and $\widetilde{\epsilon}_y = \widetilde{\sigma}_y\widetilde{\theta}_y$) are estimated in both directions.

In order to determine the feasibility and applicability of the proposed method for estimating the electron beam emittance, we made a cycle of estimates of the electron beam emittance through this technique and "noisy" angular distributions for several horizontal beam sizes. For simplicity, it was assumed that the emittances in both directions were known and were equal to ϵ_x = 0.0006 mm·mrad and ϵ_y = 0.00025 mm·mrad, which corresponds to the value of the normalized emittance $\gamma\epsilon_x \sim$ 11.7 μm·radian and is close enough to the $\gamma\epsilon_x \sim$ 10 μm·radian for the ILC collider and an electron energy of 250 GeV [4].

For the same reason, the symmetry planes of the beam coincide with the horizontal and vertical planes. The distances between the crystal and the coordinate detector are 2 and 4 m. The other conditions coincide with those used above. The dependence of $\widetilde{\epsilon}_x$ and $\widetilde{\epsilon}_y$, obtained by modeling, on the horizontal beam size is plotted in Fig. 9.

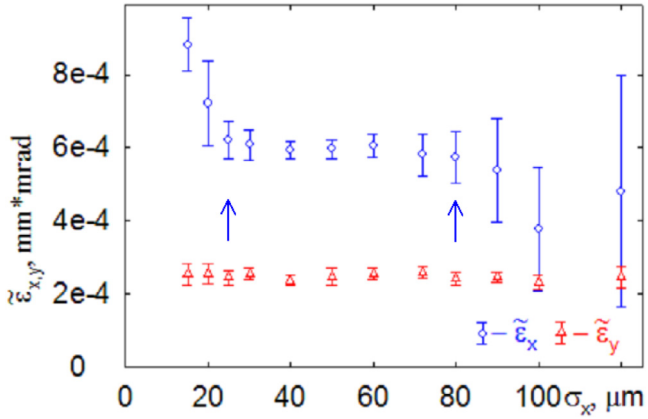

Fig. 9. Dependence of the emittance estimate on horizontal beam size. Silicon, electron energy 10 GeV, observation angle Θ_D = 32.2°, ϵ_x = 0.0006 mm·mrad, ϵ_y=0.00025 mm·mrad.

Fig. 9 shows that in the σ_x range from 25 to 80 μm, the horizontal emittances obtained by fitting coincide with the true values, while outside this range indicated by arrows, the obtained emittances deviate significantly from the true values. Moreover, in the region of small σ_x, there is a systematic shift of $\widetilde{\epsilon}_x$ to larger values, and for large sizes, that is, small divergences ($\theta_x < 7.5\mu\text{rad} \sim 0.15\gamma^{-1}$), there is a sharp increase in the fitting error.

The vertical emittance estimates behave similarly. The average value of $\widetilde{\epsilon}_y$ does not depend on the horizontal beam size, while the error in its determination increases in the regions of small and large σ_x. Since in expressions (8) and (10) the variables θ_y, σ'_y and θ_x, σ'_x are independent, varying the parameters of the vertical distribution will practically have no effect on estimates of the emittance in the horizontal plane.

To understand the reasons for this behavior of the dependences of $\widetilde{\epsilon}_x$ and $\widetilde{\epsilon}_y$ on the horizontal beam size, Fig. 10 shows the dependences of the ratio of the estimates of the vertical and horizontal beam parameters, obtained in determining the emittance, to their true values, on the horizontal beam dimensions for transverse dimensions (10a) and divergence angle (10b).

Fig. 10(a) shows that the increase in the estimate of the horizontal emittance for small beam sizes is due to the shift in the estimate of the transverse dimensions caused by a decrease in the effective divergence angle $\sigma'_x = \sigma_x/R_2$ (see Fig. 3 and its caption). For σ_x = 20 μm, the effective divergence σ'_x = 10 μrad $\sim 0.2\gamma^{-1}$. The wider applicability of the technique compared to the conditions in Fig. 3 is presumably due to the lower relief, that is, the ratio of the amplitude at the maximum to the depth of the dip, of the horizontal angular distribution of the DTR in comparison with the vertical angular distribution (see Fig. 2). For large values of σ_x, the spread in estimates of the horizontal beam size decreases and the error in determining the vertical beam size increases from 3% to 12%.

A comparison of Figs. 9 and 10(b) clearly shows that the scatter in the emittance estimates in the large σ_x region is due to the scatter in beam divergence in the horizontal direction obtained during fitting. It should be noted that the error in determining the vertical divergence is practically independent of σ_x (see Fig. 9b), that is, an increase in the error in determining the vertical emittance for large σ_x values is due only to an increase in the error in determining $\widetilde{\sigma}_y$.

To help visualize this behavior of $\widetilde{\theta}_x$, Fig. 11 shows the dependences of the ratio of the vertical and horizontal divergence estimates to the true values on the horizontal beam size, obtained for the beam sizes specified in the simulation process in both directions. Thus, the influence of the error in determining the horizontal and vertical dimensions of the beam on the error in estimating the divergence is excluded.

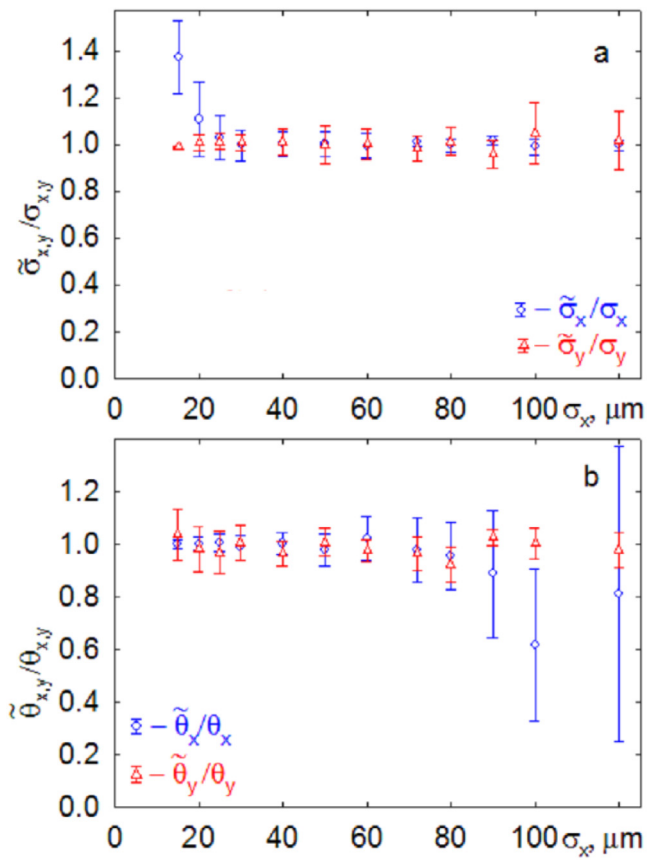

Fig. 10. Dependence of the ratios $\tilde{\sigma}_{x,y}/\sigma_{x,y}$ (a) and $\tilde{\theta}_{x,y}/\theta_{x,y}$ (b) on horizontal beam size. Silicon, electron energy 10 GeV, observation angle $\Theta_D = 32.2°$, $\epsilon_x = 0.0006$ mm·mrad, ϵ_y=0.00025 mm·mrad, σ_y=25 μm, θ_y=10 μrad.

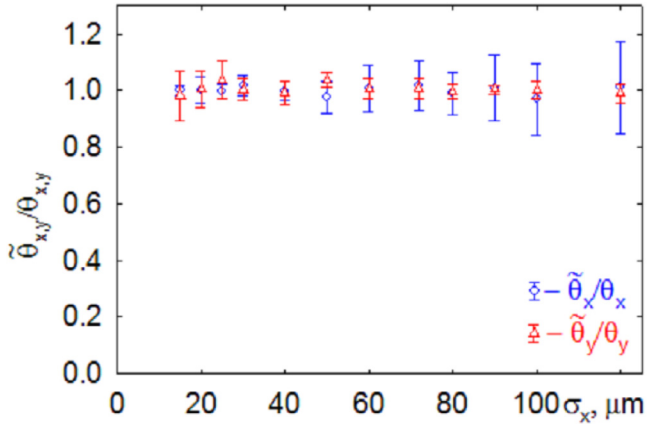

Fig. 11. Dependence of the ratios $\tilde{\theta}_{x,y}/\theta_{x,y}$ on horizontal beam size for fixed σ_x, σ_y values. Silicon, electron energy 10 GeV, observation angle $\Theta_D = 32.2°$, R_1=4 m, $\epsilon_x = 0.0006$ mm·mrad, ϵ_y=0.00025 mm·mrad, σ_y=25 μm, θ_y=10 μrad.

Fig. 11 shows that for fixed σ_x, σ_y values, estimates of the horizontal beam divergence $\tilde{\theta}_x$ coincide with the true values over the entire range of horizontal beam sizes. Consequently, the error in the horizontal emittance for small θ_x values is mainly due to the error in determining the beam size.

For $\sigma_x > 80$ μm ($\theta_x < 7.5$ μrad), that is, in the range of angles where large deviations of horizontal emittance from the true values are observed, the scatter in the estimates of the horizontal divergence ~ 10%–15% is significantly larger than for smaller values of σ_x. This is most likely because the increase in errors is due to a decrease in θ_x compared to the effective divergence $\sigma'_x = \sigma_x/R_1 > 20$ μrad. It is also related to the difference in the magnitude of the errors in comparison with the results shown in Fig. 7 for a smaller beam size and a larger distance between the crystal and the coordinate detector, which yields a value that is $\sigma'_y = \sigma_y/R_1$ ~3 μrad smaller than the vertical divergence.

The above analysis demonstrates that the proposed technique can be used to determine the emittance of an electron beam with an energy of more than 5 GeV, that is, where the PXR contribution is negligible. In the first stage, by comparing the angular distributions measured for two different distances, the beam profile is determined, that is, its transverse dimensions $\tilde{\sigma}_x$, $\tilde{\sigma}_y$ and, if necessary, the angle of rotation of the symmetry plane relative to the horizontal plane. In the second stage, according to the results of fitting the model angular distribution of DTR to the angular distribution at a larger distance, and taking into account the transverse size of the beam on the target, the values of the beam divergence $\tilde{\theta}_x$ and $\tilde{\theta}_y$ and its emittance are determined in both directions.

As the limits of applicability of the method for estimating the beam emittance, in the first approximation we can take the applicability conditions for determining the beam size and its divergence separately, that is, $\sigma'_{x,y} = \sigma_{x,y}/R_2 > 0.1\gamma^{-1}$ and $\theta_{x,y} > 0.1\gamma^{-1}$. Combining these conditions allows one to obtain the following estimate of the minimum value of the measured normalized emittance $\gamma\epsilon_{x,y} > 0.01R_2\gamma^{-1}$.

For an electron energy of 10 GeV, the same "noise" level and a smaller distance between the crystal and the coordinate detector R_2 = 1 m, we obtain the minimum measured value of the normalized emittance $\gamma\epsilon_{x,y} > 0.01R_2\gamma^{-1} \sim 0.5$ μm·radian, which is comparable to the normalized emittance of an X-ray free electron laser in both planes (~1 μm·radian) [30], the normalized horizontal emittance of the CLIC (0.66–2.4 μm·radian) [5] and is significantly higher than the value of the vertical normalized emittance of the planned electron–positron colliders ~ 30 nm·radian [4,5]. Meeting the requirement $\sigma_{x,y} > \delta$ = 10 μm increases the value of the minimum measurable normalized emittance to $\gamma\epsilon_{x,y}$ ~ 1.0–1.5 μm·radian.

In order to expand the applicability of the method, the "noise" level and the distance between the crystal and the coordinate detector should be reduced for a close position of the counter. The choice of $k = R_1/R_2 \sim 3$–5 instead of 2, as in our simulations, will reduce the contribution of the error in determining the transverse dimensions to the beam divergence and emittance determined by the proposed technique. A decrease in the pixel size of the coordinate detector should expand the applicability of the method and decrease the lower limit of the emittance, which can be measured using the proposed technique. The exact boundaries of the applicability of the method can be determined after choosing the coordinate detector and the positions where it will not affect the acceleration process and where its installation will not lead to a significant increase in cost.

As noted above, we used a model distribution of DTR (expression (2)) that was obtained under the assumption that $\Delta\theta \ll \gamma^{-1}$. If this condition is not met, then to obtain the model angular distribution of DTR $J(\vartheta'_x, \vartheta'_y)$ it is necessary to use the more precise expression (1) instead of expression (2) and explicitly take into account the effects of the Darwin table width $\Delta\theta$ and the exact form of the dependence $R(\vec{n} \to \vec{n}', \omega, \vec{g})$ (see [23,31]) on the crystal parameters and measurement conditions for the angular distribution of DTR.

This approach will smoothen the angular distribution from the monodirectional electron beam $J(\vartheta'_x, \vartheta'_y)$, which will not affect the effectiveness of the proposed technique, but may slightly change the limits of its applicability.

It should be noted that the degree of smoothening is determined by the width of the Darwin table $\Delta\theta$, which, in turn, depends on

the reflecting plane and the photon energy. Therefore, to reduce the distortions of the angular distribution of DTR, we can use the crystallographic planes (001) and (112), for which the width of the Darwin table is approximately two to three times smaller, than for the (011) plane with $\Delta\theta = 13.46$ μrad for the present geometry of observation.

Conversely, using the reflective (111) plane, as suggested in [17], the width of the Darwin table will almost triple, become comparable to γ^{-1}, and even exceed it, depending on the electron energy and the angle of observation. A more detailed analysis of the effect of the Darwin table width and the angular dependence of the reflectivity on the angular distribution of the diffracted transition radiation is beyond the scope of the proposed study. A study investigating these issues is currently underway, the results of which will be presented soon.

7. Conclusions

The emittance of a beam of electrons with energies above 5 GeV $\epsilon_{x,y}$, where the contribution of parametric X-ray radiation is negligible and the beam size is about 15-20 μm and higher, can be determined from measurements of the angular distributions of diffracted transition radiation of relativistic electrons in thin crystals for two different distances between the source and the coordinate detector.

The transverse dimensions of the beam $\sigma_{x,y}$ are determined from the results of fitting the distribution for a smaller distance by convolving the distribution for a larger distance with a two-dimensional Gaussian distribution, the parameters of which are unambiguously related to the dimensions of the beam and the distances between the crystal and the detector as outlined in the method in [20]. The limit of applicability of this technique is the condition $\sigma_{x,y}/R_2 > 0.1\gamma^{-1}$, where R_2 is a shorter distance.

An additional requirement is the fulfillment of the condition for the ratio of the characteristic beam size to the detector size, $\sigma \geq \delta$, where δ is the pixel size of the coordinate detector. The method for estimating the electron beam size [20] is model-independent and does not require exact knowledge of the beam divergence or the degree of the crystal structure perfection. The technique makes it possible to determine not only the size of the beam on the target, but also its symmetry plane's rotation angle with respect to the horizontal and vertical planes.

The beam divergence $\theta_{x,y}$ is determined from the results of fitting the angular distribution measured for a larger distance by convolution of the model angular distribution of diffracted transition radiation with a two-dimensional Gaussian distribution describing a diverging electron beam, taking into account the transverse dimensions and, if necessary, the beam's rotation angle obtained in the first stage of processing.

The present approach allows the estimation of the divergence of an electron beam with known sizes $\sigma_{x,y}$ in both directions $\theta_{x,y}$ with an error of no more than 5%–10% if the condition $\theta_{x,y} > 0.1\gamma^{-1}$ is satisfied. In order to reduce the error in the divergence, it is desirable to satisfy the condition $\sigma_{x,y}/R_1 < \theta_{x,y}$. When the condition $\sigma'_{x,y} = \sigma_{x,y}/R \ll \theta_{x,y}$ is satisfied, the technique enables the determination of not only the beam divergence, but also the tilt angle of its plane symmetry about the vertical and horizontal planes.

In the case of an extended electron beam and measurements for different distances between the crystal and the coordinate detector in order to determine the beam emittance, both conditions must be satisfied: $\sigma'_{x,y} = \sigma_{x,y}/R_2 > 0.1\gamma^{-1}$ and $\theta_{x,y} > 0.1\gamma^{-1}$. The lower boundary of the region of applicability of the technique is determined by the pixel size of the coordinate detector and the attainable range of distances between the crystal and the detector.

CRediT authorship contribution statement

Yu.A. Goponov: Software, Validation. **R.A. Shatokhin:** Software, Validation. **K. Sumitani:** Validation. **Y. Takabayashi:** Conceptualization, Writing - review & editing. **I.E. Vnukov:** Conceptualization, Software, Writing - original draft, Supervision.

Declaration of competing interest

The authors declare that they have no known competing financial interests or personal relationships that could have appeared to influence the work reported in this paper.

Acknowledgments

This work was supported in part by JSPS KAKENHI, Japan Grant Number JP26400304.

References

[1] R.B. Fiorito, Proceedings of PAC09, 2009, p. 741.
[2] J. Urakawa, H. Hayano, K. Kubo, S. Kuroda, N. Terunuma, M. Kuriki, T. Okugi, T. Naito, S. Araki, A. Potylitsyn, G. Naumenko, P. Karataev, N. Potylitsyna, I. Vnukov, T. Hirose, R. Hamatsu, T. Muto, M. Ikezawa, Y. Shibata, Nucl. Instrum. Methods Phys. Res. Sect. A 472 (2001) 309.
[3] G. Kube, H. Backe, W. Lauth, H. Schöpe, Proceedings of DIPAC2003, 2003, p. 40.
[4] ILC Technical Design Report, 2013.
[5] A Multi-TeV Linear Collider Based on CLIC Technology: CLIC Conceptual Design Report, 2012.
[6] H. Loos, et al., Proceedings of FEL08, 2008, p. 485.
[7] R. Fulton, J. Haggerty, R. Jared, R. Jones, P. Kadyk, C. Field, W. Kozanecki, W. Koska, Nucl. Instrum. Methods Phys. Res. Sect. A 274 (1989) 37.
[8] M. Harrison, et al., Proceedings of FEL2013, 2013, p. 276.
[9] T. Shintake, Nucl. Instrum. Methods Phys. Res. Sect. A 311 (1992) 453.
[10] Yu.A. Goponov, M.A. Sidnin, K. Sumitani, Y. Takabayashi, I.E. Vnukov, Nucl. Instrum. Methods Phys. Res. Sect. A 808 (2016) 71.
[11] Yu.A. Goponov, R.A. Shatokhin, K. Sumitani, V.V. Syshchenko, Y. Takabayashi, I.E. Vnukov, Nucl. Instrum. Methods Phys. Res. Sect. A 885 (2018) 134.
[12] A. Gogolev, A. Potylitsyn, G. Kube, J. Phys. Conf. Ser. 357 (2012) 012018.
[13] Y. Takabayashi, Phys. Lett. A 376 (2012) 2408.
[14] Yu.A. Goponov, S.A. Laktionova, O.O. Pligina, M.A. Sidnin, I.E. Vnukov, Nucl. Instrum. Methods Phys. Res. Sect. B 355 (2015) 150.
[15] S.V. Blazhevich, G.A. Grazhdankin, R.A. Zagorodnyuk, A.V. Noskov, Nucl. Instrum. Methods Phys. Res. Sect. B 355 (2015) 170.
[16] I. Chaikovska, R. Chehab, X. Artru, A.V. Shchagin, Nucl. Instrum. Methods Phys. Res. Sect. B 402 (2017) 75.
[17] S.V. Blazhevich, M.V. Bronnikova, A.V. Noskov, Phys. Lett. A 384 (2020) 126321.
[18] P. Rullhusen, X. Artru, P. Dhez, Novel Radiation Sources using Relativistic Electrons, World Scientific, Singapore, 1999.
[19] I.D. Feranchuk, A.V. Ivashin, J. Phys. (Paris) 46 (1985) 1981.
[20] I.E. Vnukov, Y.A. Goponov, M.A. Sidnin, R.A. Shatokhin, K. Sumitani, Y. Takabayashi, J. Surf. Invest. 13 (2019) 515.
[21] Yu.A. Goponov, S.A. Laktionova, R.A. Shatokhin, M.A. Sidnin, K. Sumitani, Y. Takabayashi, I.E. Vnukov, Phys. Rev. Accel. Beams 22 (2019) 082803.
[22] Y.N. Adischev, S.N. Arishev, A.V. Vnukov, A.V. Vukolov, A.P. Potylitsyn, S.I. Kuznetsov, V.N. Zabaev, B.N. Kalinin, V.V. Kaplin, S.R. Uglov, A.S. Kubankin, N. Nasonov, Nucl. Instrum. Methods Phys. Res. Sect. B 201 (2003) 114.
[23] K.-H. Brenzinger, et al., Z. Phys. A 358 (1997) 107.
[24] S.A. Laktionova, O.O. Pligina, M.A. Sidnin, I.E. Vnukov, J. Phys. Conf. Ser. 517 (2014) 012020.
[25] A.P. Potylitsin, V.A. Verzilov, Phys. Lett. A 209 (1995) 380.
[26] G.M. Garibian, C. Yang, X-ray Transition Radiation, Akad. Nauk Armenia, Yerevan, 1983, (in Russian).
[27] High-Resolution X-ray Camera, http://www.proxivision.de/datasheets/X-ray-Camera-HR25-x-ray-PR-0055E-03.pdf..
[28] G. Kube, C. Behrens, A.S. Gogolev, Yu.P. Popov, A.P. Potylitsyn, W. Lauth, S. Weisse, Proceedings of IPAC2013, 2013, p. 491.
[29] Yu.A. Goponov, R.A. Shatokhin, M.A. Sidnin, K. Sumitani, Y. Takabayashi, I.E. Vnukov, I.S. Volkov, JINST 15 (2020) C04025.
[30] The European X-ray Free-Electron Laser Technical Design Report, DESY 2006-097, 2007.
[31] R. James, The Optical Principles of the Diffraction of X-Rays, G. Bell and Sons, London, 1958.